

## Longitudinal Single-Bunch Instability Studies for Sirius

F. H. de Sá

*Accelerator Physics Group, Brazilian Synchrotron Light Laboratory (LNLS)  
 fernando.sa@lnls.br*

In this work the longitudinal dynamics of the Sirius storage ring is analyzed using tracking codes applied to the parameters of its first phase of operation. As a result, an effective simplified impedance model based on resonators is built for the machine and a simple theory to explain the mechanism that drives noise in tracking simulations is created.

*Keywords:* Sirius; impedance budget; instabilities

### 1. Introduction

Sirius is a 3 GeV fourth-generation light source being built in Campinas, Brazil, by the Brazilian Synchrotron Light Laboratory (LNLS). The status of the construction, as well as informations about the magnetic lattice and radiation sources, can be found elsewhere<sup>1-3</sup>. The standard vacuum chamber of the ring will be round and made of copper, with an inner radius of 12 mm. The whole ring's vacuum chamber will be NEG coated, and two operation phases are planned, with corresponding 100 mA and 350 mA (with Landau cavity) nominal currents for uniform filling. Table 1 shows the main parameters of the phase 1 of the storage ring that are relevant for this study.

In previous works<sup>4,5</sup> the impedance-related collective effects in Sirius were reported using a very preliminary impedance budget, which took into account the resistive-wall impedance and a broad-band resonator (BBR) model for the geometric impedance. Since then, several components of the storage ring had their impedance calculated with 3D electromagnetic codes (mostly with GdfidL<sup>6</sup>) such

Table 1. Main Parameters of the Sirius Storage Ring.

Parameter	Symbol	Values	Unit
Energy	$E_0$	3.0	GeV
Circumference	$L_0$	518.4	m
Revolution period	$T_0$	1.73	$\mu$ s
Harmonic number	$h$	864	
Momentum compaction	$\alpha$	$1.7 \times 10^{-4}$	
Energy loss per turn (dipoles)	$U_0$	473	keV
Natural energy spread	$\sigma_\delta$	$8.5 \times 10^{-4}$	
Damping rates (H/V/L)	$\alpha_{x/y/z}$	59.2/45.5/77.5	Hz
Nominal total current	$I_0$	100	mA
Voltage gap	$V_0$	3.0	MV
Natural bunch length	$\sigma_z$	2.5(8.2)	mm(ps)
Synchrotron Tune	$\nu_z$	$4.6 \times 10^{-3}$	

as the ones described in Refs. 7–9. Some other components, which have not been designed in detail, and consequently do not have a 3D evaluation carried out, have had their impedance estimation refined. Instead of BBR models, 2D codes such as ECHO2D<sup>10,11</sup> were used to simulate approximate geometries, which preserved the main parameters of the structure under analysis.

With this improved impedance budget the instability thresholds for Sirius were re-evaluated, as described in Ref. 12, using frequency domain codes based on Suzuki's<sup>13,14</sup> solution of the linearized Fokker-Planck equation for the longitudinal and transverse planes assuming a gaussian bunch (i.e., neglecting potential-well distortions), that were extended to deal with the multi-bunch uniform filling case. Since then, a tracking code was developed and the Haissinski solver was revised.

In this work the longitudinal tracking results for Sirius with the total impedance budget will be presented. In Sec. 2 the methods used in the Haissinski solver and in the tracking code are briefly described, in Sec. 3 the construction of an impedance model for the longitudinal plane based only on resonators is treated and in Sec. 4 noise issues with the first simulations are discussed, where a simple theory to explain its mechanism is introduced.

## 2. Description of the Methods

### 2.1. Haissinski Solver

The Haissinski equation can be written in the following form,  $\rho(z) = \mathcal{H}(\rho, z)$ , where

$$\mathcal{H}(\rho, z) = B \exp \left( \frac{q}{\alpha L_0 E_0 \sigma_\delta^2} \left( U_{\text{cav}}(z) - I_b T_0 \int_{-\infty}^{\infty} dz' W'_0(z - z') \rho(z') \right) \right),$$

with  $B \in \mathbb{R} \mid \int_{-\infty}^{\infty} dz \mathcal{H}(\rho, z) = 1$ ,

(1)

$q$  is the electron charge,  $I_b$  is the bunch current and  $W'_0$  is the total longitudinal wake function.

To solve this equation an iterative approach was adopted: starting from a very low  $I_b$  and an initial guess

$$\rho_0^{I_b}(z) = A \exp \left( \frac{q U_{\text{cav}}(z)}{\alpha} L_0 E_0 \sigma_\delta^2 \right), \quad \text{with } A \in \mathbb{R} \mid \int_{-\infty}^{\infty} dz \rho_0^{I_b}(z) = 1, \quad (2)$$

we iterate

$$n = 1 : \rho_n^{I_b}(z) = \mathcal{H}(\rho_0^{I_b}, z), \quad n > 1 : \rho_n^{I_b}(z) = \mathcal{H} \left( \frac{\rho_{n-1}^{I_b} + \beta \rho_{n-2}^{I_b}}{1 + \beta}, z \right) \quad (3)$$

where  $\beta$  is a positive convergence-control variable. For each iteration the difference

$$d_n^{I_b} = \int_{-\infty}^{\infty} dz \left( \rho_n^{I_b} - \rho_{n-1}^{I_b} \right)^2 \quad (4)$$

is calculated and compared to a threshold,  $\epsilon$ . When  $d_{n_c}^{I_b} < \epsilon$ , convergence is assumed and we set  $\rho^{I_b} = \rho_{n_c}^{I_b}$ . Then, the current is incremented by a small value  $I_b + \Delta I$ ,

with  $\Delta I \ll I_b$ , and the process is repeated with the initial guess  $\rho_0^{I_b+\Delta I} = \rho^{I_b}$ . Note that this method does not require the wakes to respect causality and can also be applied to non-parabolic RF cavity potentials.

This implementation was benchmarked with the results presented in Ref. 15 for the inductive and resistive impedances<sup>a</sup>. For the capacitive (positive inductance) the code fails to converge above a given threshold, close to the well-known singularity point of such impedance<sup>16</sup>. However this was not a problem for all the practical cases studied here.

## 2.2. Tracking Code

The structure of the tracking code used is very similar to the one described in Ref. 5, with the additional feature of including damping and quantum excitation terms for the single particle dynamics. Wake field kicks can be included in two different ways:

- **General Wakes:** In this case the wakes do not need to respect the causality condition and are passed to the code as interpolation tables. The code uses the Particle In Cell (PIC) approach, where the total simulation length of the longitudinal direction,  $L_c$ , is segmented in  $N_c$  intervals and the approximate beam distribution is calculated from the number of macroparticles in each cell. Then, the convolution theorem is used to calculate the kick curve<sup>17</sup>, which is interpolated according to each particle's position;
- **Resonators:** The parameters of the resonators,  $(R_s, \omega_r, Q)$ , are used as input. The code does not use the PIC approach, each of the  $N_p$  macroparticles being simulated interact with each other and the wake is calculated through the sum of the potentials left by each particle in each resonator.

Note that in the second method  $N_p$  is the only variable to be tested for the analysis of the convergence of the results, while for the first method the additional variable  $N_c$  is also important. A natural choice for the number of slices is to make it large enough that the grid length satisfies the Nyquist theorem for the highest relevant frequency of the impedance used in tracking,

$$\Delta z_c = L_c/N_c > \frac{2}{f_{\max}}, \quad (5)$$

this way, the convergence of the results will depend only on the number of macroparticles used.

This code was benchmarked with SPACE<sup>17</sup> and Elegant<sup>18</sup>.

---

<sup>a</sup>Since the code cannot handle wake functions that are given by distributions, such as the  $\delta'(z)$  and the  $\delta(z)$  of the inductive and resistive wakes, respectively, the functions used for the simulation in these cases were their convolution with a very small ( $\sigma_z = 20\mu\text{m}$ ) gaussian bunch.

Table 2. BBR model with 10 resonators of the Sirius longitudinal impedance budget.

$f_R$ [GHz]	716.2	206.9	138.4	79.6	57.3	35.0	17.5	17.8	11.9	9.2
$R_s$ [k $\Omega$ ]	30.0	6.5	2.0	2.0	2.5	2.5	1.7	3.0	4.0	20.0
$Q$	0.7	1.3	4.0	1.0	4.5	3.0	1.0	24.0	24.0	100.0

### 3. Impedance Model

Table 2 shows the BBR model of the Sirius longitudinal impedance budget. The very high frequency BBR, the first in the table, is due to the NEG coated vacuum chamber, which has a very large inductive impedance at low frequencies, being the major contributor for the bunch lengthening. Moreover, note that the last three resonators have a fairly large  $Q$  factor. They are originated from the bellows and the BPMs of the machine, and, as explained below, are important to account for the behavior of the beam above the threshold of the microwave instability.

This impedance model was built by fitting the total impedance budget and refined based on comparisons of the instabilities thresholds predicted by both of them in frequency domain, on the bunch-lengthening and synchrotron phase shift as function of the bunch current and also on the behavior of the distribution above the threshold, calculated by tracking. In this process, it was noted that including only the first seven BBR is enough to explain the bunch-lengthening effects and the threshold for the microwave instability, but only with all ten resonators it is possible to reproduce the behavior above the threshold, as shown in Fig. 1 and Fig. 2.

### 4. Noise in tracking simulations

In order to simulate correctly the high frequency BBR of the impedance model, fulfilling the condition imposed by the Nyquist theorem expressed in Eq. (5), it was necessary to set  $\Delta z_c = 2\mu\text{m}$ . Figure 3 shows the results of tracking with the impedance budget of the Sirius storage ring for different numbers of macroparticles in comparison with the behavior predicted by the Haissinski solver and Fig. 4 shows the integrated power spectrum of the kick received by an arbitrary particle in the bunch. Note that even with a number of particles as high as 1 M particles, there is still a strong influence of noise, and only with 10 M particles the results seem to have converged, where the onset of an instability is noted at approximately 3 mA. Such results motivated us to try to understand the mechanism that drives this behavior.

Given a longitudinal density distribution  $\rho(z)$ , the number of particles in a small interval  $\Delta z$  centered at the position  $z$ ,  $N_l(z)$ , is a random variable that follows a binomial distribution. Thus, considering that there are  $N_p$  particles in the bunch, we have

$$\langle N_l \rangle = \rho(z)\Delta z N_p \quad \text{and} \quad \text{var}(N_l) \approx \rho(z)\Delta z N_p, \quad (6)$$

where  $\langle \cdot \rangle$  and  $\text{var}(\cdot)$  denotes average and variance, respectively, being the latter a measure of the fluctuations in the bunch due to the finite number of particles. If

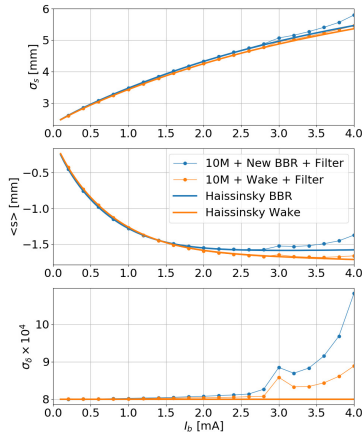


Fig. 1. Bunch length, synchrotron phase shift, and energy spread as function of the single bunch current for the BBR model and the real wake of the machine, calculated by tracking and using the Haissinsky solver. Note that both impedance models agree very well and predict the threshold of the microwave instability at  $\approx 2.7\text{mA}$ .

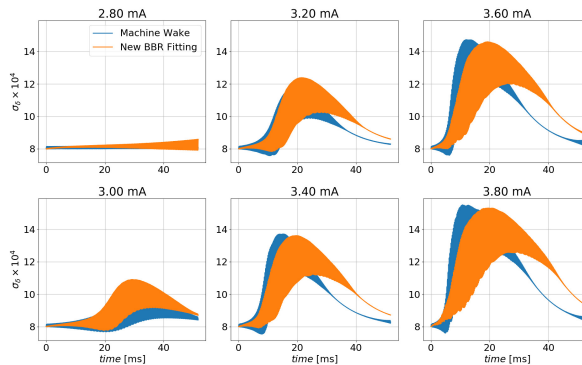


Fig. 2. Time evolution of the energy spread in tracking simulations for different currents above the threshold of the microwave instability, showing one cycle of instability growth, saturation and damping. This sawtooth-like behavior repeats indefinitely and seriously compromises the quality of the radiation emitted. Note the good agreement between the behavior predicted by the BBR model and the detailed computed wake of the machine. It is interesting that the BBR have higher growth rates at lower currents, 2.8 and 3.0 mA, but for higher currents the other model predict faster growths. Such behavior should be investigated further.

the particles were static, this fluctuation would also be, but, as they are moving due to the longitudinal dynamics of the storage ring, these fluctuations are constantly changing. For very small  $\Delta z$ , the value of  $N_l(z)$  changes very fast, but as  $\Delta z$  increases, this characteristic time becomes increasingly large.

It is possible to estimate the length scale where the behavior of the variance changes by considering the number of turns it takes for the stored particles to complete one oscillation in the longitudinal phase space, which is  $1/\nu_z$ . This means that, on average, the longitudinal position of each particle differs from its position in the last turn by  $\Delta z_L \approx 4\nu_z\sigma_z$ . Consequently, for scales below or on the order of this length, the fluctuations of the particle distribution changes in a turn by turn basis.

Now, let's consider there is a wake function  $W(z)$  that is constant in a small interval  $\Delta z_W \approx \Delta z_L$  behind the source particle and zero outside this interval. Then, any particle inside the bunch would receive random kicks  $K = eI_b T_0 W N_l / N_p$ . The average of this kick varies slowly in time, because it depends on the evolution of the density distribution, but the variance, given by

$$\text{var}(K) = (qI_b T_0 W)^2 \frac{\text{var}(N_l)}{N_p^2} \approx (qI_b T_0 W)^2 \frac{\Delta z_W}{\sqrt{2\pi e} N_p}, \quad (7)$$

varies from turn to turn, where in the last step it was assumed  $z \approx \sigma_z$  and that the distribution is gaussian,  $\rho(\sigma_z) = 1/\sqrt{2\pi e}\sigma_z$ . Summarizing, this mechanism

introduce a random variation of the energy of the particles in a turn by turn basis, similarly to the quantum excitation process due to radiation emission. This means that it should change the energy spread of the beam by

$$\Delta\sigma^2 = \sigma_\delta^2 - \sigma_{\delta 0}^2 \approx \frac{\text{var}(K)/E_0^2}{\alpha_z T_0(2 - \alpha_z T_0)} = \left( \frac{qI_b T_0 W}{E_0} \right)^2 \frac{\Delta z_W}{\sqrt{2\pi} e N_p} \frac{1}{\alpha_z T_0(2 - \alpha_z T_0)}. \quad (8)$$

Figure 5 shows the energy spread variation from Sirius tracking simulations multiplied by  $N_p \sigma_s / I_b^2$ . Note that according to Eq. (8) this quantity should depend only on the storage ring properties and on the wake characteristics,  $(W, \Delta z_W)$ , and, therefore should be an horizontal straight line. Note that this is the behavior for the 100 k and 1 M particles curve and that the 10 M curve deviates from this behavior above 2 mA, but approaches the same baseline of the others for lower currents. This deviation is understood when the simulation with 50 M particles is analysed, where the real microwave instability dominates the scaling. Other two simulations with 1 M particles are also shown, one without the high frequency resonator, where we note the real instability also happens, with approximately the same characteristics of the 50 M particles curve, and another with a filtered wake. This filter consists in convolving the total wake function with a small gaussian bunch ( $\sigma_z = 40\mu\text{m}$ ) and using this effective wake as input for the simulation, this approach changes the short range wake by filtering out high frequencies of the impedance spectrum. Even though this filtered model has a smaller baseline than the other curves, it was not enough to predict the instability at  $\approx 2.5$  mA, due to the additional energy

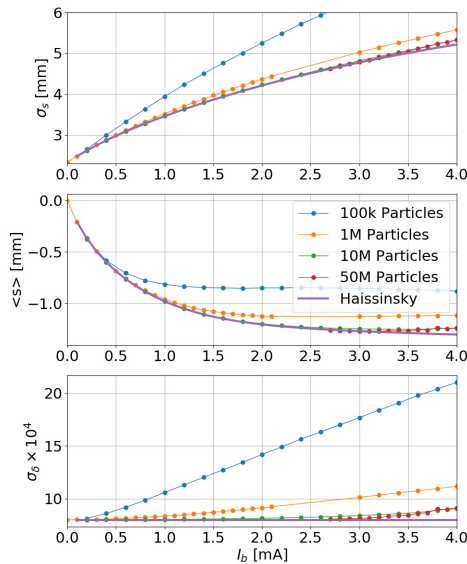


Fig. 3. Tracking results, showing the effect of noise as a function of the number of macroparticles used in the simulation.

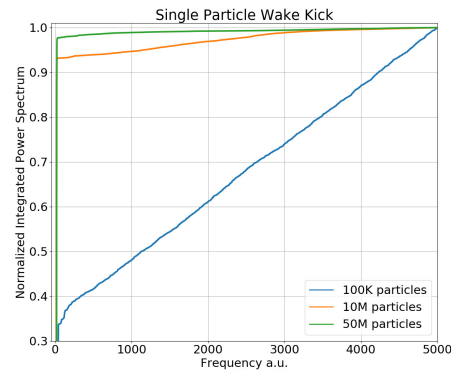


Fig. 4. During tracking simulations one particle is followed and its position in phase space and kick received by the wake are stored for each turn. The figure above shows the integrated power spectrum of the kick as a function of the frequency for simulations with 4 mA in the bunch. As the number of particles simulated increases, the energy is concentrated in very low frequencies, which corresponds to the synchrotron frequency.

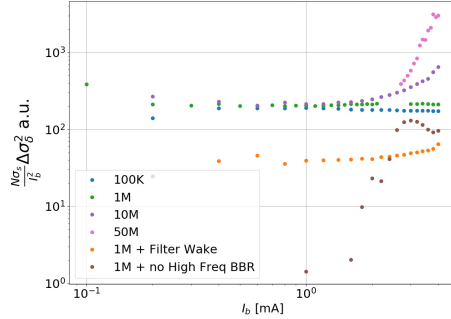


Fig. 5. Energy spread increase in simulations multiplied by  $N_p \sigma_s / I_b^2$ . The curves 100 k, 1 M, 10 M and 50 M were performed with the same wake function, while for curve 1 M + Filter Wake a convolution with a  $40\mu\text{m}$  gaussian bunch was applied to the wake and for the other curve, the resonator with highest frequency presented in Tab. 2 was not used. Note how the baselines change depending of the wake function used.

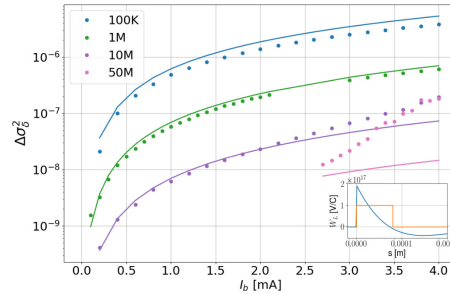


Fig. 6. Dots represents the energy spread increase in simulations with the same wake function (represented by the blue curve in the small graphic) and lines are the prediction of Eq. (8) using a constant model for the wake (orange line in the small graphic), with  $W = 1 \times 10^7 \text{V/C}$  and  $\Delta z_W = 80\mu\text{m}$ .

spread introduced by the noise, like the unfiltered simulations with 100 k and 1 M particles. While Fig. 5 shows that Eq. (8) qualitatively explains the energy spread increase induced by noise in simulations, Fig. 6 shows that, even though several approximations were performed in its deduction, it can be used to quantitatively estimate the number of particles needed to avoid such problems.

Even though all the simulations presented here were performed with the General Wakes mode of the tracking code, which uses the PIC method, the same results were also observed for tracking the pure Resonators. This indicates that the effect described above is not related to the PIC method, but is a limitation of the physical system used to replace the real one in the simulations. The reduced number of particles increase the fluctuations that already exist in the real beam and, as Eq. (8) suggests, would also induce energy spread increase in the physical system if the wake were  $\approx 100$  times stronger.

## 5. Conclusions

In this work it was shown that the longitudinal BBR model explains well the behavior of the bunch in terms of energy loss, bunch-lengthening and time evolution above the microwave instability threshold, that is predicted to be approximately 2.7 mA for Sirius. Also, the difficult task of simulating very high frequency wakes was analyzed and a simple theory to explain the noise it introduces in the results were developed. Such a theory proved to be helpful in estimating the tracking parameters for the simulations. In the next step of the work, the CSR wake will be introduced in the impedance model and tracking simulations will be extended to the transverse planes.

## Acknowledgments

I would like to thank the LNLS Accelerator Physics Group members for their support in the development of the codes, fruitful discussions and careful review of this paper. I also thank Ryan Lindberg for sharing APS impedance data and Elegant results for benchmarking of the tracking code and Gabriele Bassi for doing the same with SPACE and for the discussions. Thanks to Simone Di Mitri and all the organizers of the workshop for the invitation, the gracious reception at Arcidosso and the patience to wait and accept this delayed contribution.

## References

1. Sirius Official Documentation, <https://wiki-sirius.lnls.br>
2. L. Liu and H. Westfahl Jr., Towards diffraction limited storage ring based light sources, In: *Proc. of IPAC'17*, (Copenhagen, Denmark, May 2017).
3. L. N. P. Vilela, L. Liu, X. R. Resende and F. H. de Sá, Studies of Delta-type undulators for Sirius, In: *Proc. of IPAC'17*, (Copenhagen, Denmark, May 2017).
4. F. H. de Sá, L. Liu, H. O. C. Duarte, X. R. Resende and N. Milas Study of collective beam instabilities for Sirius, In: *Proc. of IPAC'14*, (Dresden, Germany, May 2014), pp. 1653–1655.
5. F. H. de Sá, L. Liu, X. R. Resende and N. Milas, Stabilities thresholds and tune shift estimation for Sirius, In: *Proc. of IPAC'15*, (Richmond, USA, May 2015), pp. 70–72.
6. GdfidL Web Site, <http://www.gdfidl.de/>.
7. H. O. C. Duarte, L. Sanfelici and S. R. Marques, Design and impedance optimization of the Sirius BPM button, In: *Proc. of IBIC13*, (Oxford, UK, Sep. 2013), pp. 365–368.
8. H. O. C. Duarte, L. Liu and S. R. Marques, Evaluation and attenuation of Sirius components impedance, In: *Proc. of IPAC'17*, (Copenhagen, Denmark, May 2017).
9. H. O. C. Duarte, T. M. Rocha, F. H. de Sá, L. Liu and S. R. Marques, Analysis and countermeasures of wakefield heat losses for Sirius, In: *Proc. of IPAC'17*, (Copenhagen, Denmark, May 2017).
10. I. Zagorodnov and T. Weiland, TE/TM field solver for particle beam simulations without numerical Cherenkov radiation, *Phys. Rev. ST-AB*, Vol. 8, p. 042001, (April 2005).
11. I. Zagorodnov, K. L. F. Bane and G. Stupakov, Calculation of wakefields in 2D rectangular structures, *Phys. Rev. ST-AB*, Vol. 18, p. 104401, (Oct. 2015).
12. H. O. C. Duarte, T. M. Rocha, F. H. de Sá, L. Liu and S. R. Marques, Analysis and countermeasures of wakefield heat losses for Sirius, In: *Proc. of IPAC'17*, (Copenhagen, Denmark, May 2017).
13. T. Suzuki, Theory of longitudinal bunched-beam instabilities based on the Fokker-Planck equation, *Part. Accel.*, Vol. 14 pp. 91–108, (1983).
14. T. Suzuki, "Fokker-planck theory of transverse mode-coupling instability", *Part. Accel.*, Vol. 20, p. 79–96, (1986).
15. K. L. F. Bane, R. D. Ruth, "Bunch Lengthening Calculations for the SLC Damping Rings", *Proc. of PAC'89* pp. 789–791, (1989).
16. Y. Shobuda, K. Hirata, "The Existence of a Static Solution for the Haissinski Equation with Purely Inductive Wake Force", *Part. Accel.*, Vol. 62, p. 165–177, 1999.
17. G. Bassi, A. Blednykh, V. Smaluk, "Self-consistent simulations and analysis of the coupled-bunch instability for arbitrary multibunch configurations", *Phys. Rev. Acc. and Beams*, Vol. 19, n. 2, p. 24401, (2016).
18. M. Borland, "Elegant: A flexible SDDS-compliant code for accelerator simulation", *Proc. of ICAP'2000*, (Darmstadt, Germany, 2000).